# Experimental Investigation on a Modular Glass Fibre Reinforced Polymer Composite Sandwich System

S. Satasivam, Y. Bai* and X.L. Zhao

*Department of Civil Engineering, Monash University, Wellington Rd, Clayton, Victoria, 3180, Australia (*E-mail: yu.bai@monash.edu)*

## ABSTRACT

Fibre reinforced polymer (FRP) sandwich systems have been used successfully in aerospace and marine engineering, and have great potential for use in civil infrastructure. FRP composites, particularly if glass fibres are used (i.e. GFRP), further exhibit advantageous environmental characteristics such as low energy consumption and low carbon dioxide emissions, but are however associated with a relatively low elastic modulus. This paper describes an innovative modular assembly system of GFRP sandwich structures used for structural construction. Built-up beam or slab modular sections consisting of GFRP standard pultruded I or box profiles are incorporated between two GFRP plates to form a sandwich structure, which can then be assembled in the transverse direction through adhesive bonding and/or mechanical bolting. The sandwich configuration allows for an increase in the sectional inertial moment, therefore improving the stiffness at the structural level by compensating for its low material elastic modulus. This structural system further provides greater flexibility in designing beam and slab systems by allowing the adjustment of various geometric parameters. A modular sandwich beam was prepared in this way and tested under four-point bending. The load carrying capacity of the specimen was evaluated and the connection detail and the degree of composite action were investigated.

## KEYWORDS

Glass Fibre Reinforced Polymer (GFRP); Adhesive bonding; Composite action; Modular system; Sandwich structure

## INTRODUCTION

Fibre reinforced polymer (FRP) composites have been used increasingly in civil applications due to their favourable properties such as their low weight, high strength and corrosion resistance. FRP composites, particularly if glass fibres are used (i.e. glass fibre reinforced polymers, GFRP), also exhibit excellent environmental characteristics such as low thermal conductivity, low energy consumption and low carbon dioxide emissions compared to concrete and steel (Halliwell, 2010). Furthermore, thanks to pultrusion technology, the cost of FRP manufacture has been reduced significantly. In civil engineering applications the use of composite materials as load carrying structural members is emerging.

However, in comparison to steel, GFRP materials are associated with a low material stiffness resulting from a low E-modulus (10% of the elastic modulus of steel). This makes the serviceability design of GFRP structures even more critical than the strength design (Bakis *et al.* 2002). Excessive deflection and vibration must be controlled within serviceability limit criteria. Improving the stiffness of GFRP structures at the structural level via sandwich construction may be a solution, since a sandwich system presents an improved inertial moment (I) and therefore compensates for a relatively low E-modulus. Research has been conducted on pultruded web flange sandwich GFRP decks for bridge construction. Such GFRP decks, which can be of a built-up, cellular or honeycomb

cross-section, is connected via shear studs and/or adhesive to supporting steel girders. Experimental results indicate that GFRP bridge decks provide sufficient strength and stiffness (Johnson *et al.*, 1990; Foster *et al.*, 2000; Turner *et al.*, 2004; Jeong *et al.*, 2007). Built-up bridge decks made from pultruded GFRP components were fabricated and tested (Hayes *et al.*, 2000; Zhou *et al.*, 2005; Liu *et al.*, 2008). In this system, a series of square tubes were bonded at their webs and then sandwiched between two flat plates and connected together via adhesive bonding. Through rods (either fibre or steel bolts) were placed transverse to the square tubes to provide clamping pressure, and the bridge decks were connected to supporting steel girders via mechanical bolts. Under flexural loads, failure occurred within the FRP material and was localised just under the loading patches. Failure was not seen in the adhesive bonds, indicating that the bonding of GFRP components is a sufficient means of connection. These experiments show that sandwich structures made from GFRP composites is viable for civil construction. However, the square tubes adhesively bonded to each other require the use of through-rods to keep them aligned whilst the adhesive was curing. These rods did not improve the overall strength and stiffness of the deck, but introduced localised stress concentrations at cut-out areas in the system. In addition, such a sandwich deck design did not allow for a variation in the spacing between square tubes or the type of cross-section of the web component.

Proper design of the shear connection is essential for full load transfer between the web and face sheets. Research into the shear connection between steel and pultruded GFRP panels indicated that adhesive bonds provided full composite action, as evidenced by the investigations on two pultruded GFRP bridge deck systems (DuraSpan® made by Martin Marietta Composites USA and Asset® made by Fiberline Denmark) adhesively bonded to steel girders in Keller and Gürtler (2005a, b). It has also been shown that full composite action can be provided by shear studs at the serviceability limit state, as demonstrated by Keelor *et al.* (2004) and Moon and Gillespie (2005). However, the shear studs used in these experiments required the careful placement of grout around the bolts. Shear studs without the use of grout was investigated by Davalos *et al* (2011), where it was found that only partial composite action was achieved between the FRP deck and the supporting steel girder. Sotiropoulous (1994) also found that the degree of composite action is limited when using steel bolts alone. These forms of shear connections, and their associated design considerations, can be applicable to the shear connection between GFRP components within a sandwich system.

This paper proposes a modular assembly system of GFRP sandwich structures used for structural construction. A sandwich beam consisting of flat panels and pultruded GFRP box sections was prepared. The sandwich components were joined together using epoxy adhesive. The sandwich beam was tested under four-point bending up to failure. Based on the experiments, the serviceability limit state and the load carrying capacity of the beam were evaluated and the failure mode was identified. Axial strains on the top and bottom facesheets were measured to characterise the strain distribution along the width of the beam. In addition, the connection detail and the degree of composite action were further investigated.

## CONCEPTUAL DESIGN

In this design, built-up beam or slab sections consisting of GFRP standard pultruded I or box profiles are incorporated between two GFRP plates to form a sandwich structure. As a modular unit, it can then be assembled in the transverse direction through adhesive bonding and/or mechanical bolting (as shown in Figure 1). The assembled sandwich unit has an increased second moment of inertia, compensating for its low elastic modulus, and hence the bending stiffness of the structure is enhanced. Compared to pre-existing pultruded GFRP decks, these structural units provide greater flexibility in designing beam and slab systems by allowing the adjustment of various geometric parameters such as the width and thickness of the flat panels, the spacing between adjacent webs, and the type and size of the web-sections. Such a modular sandwich system further allows a high

degree of prefabrication and rapid on-site installation for construction of large-scale beam and slab systems.

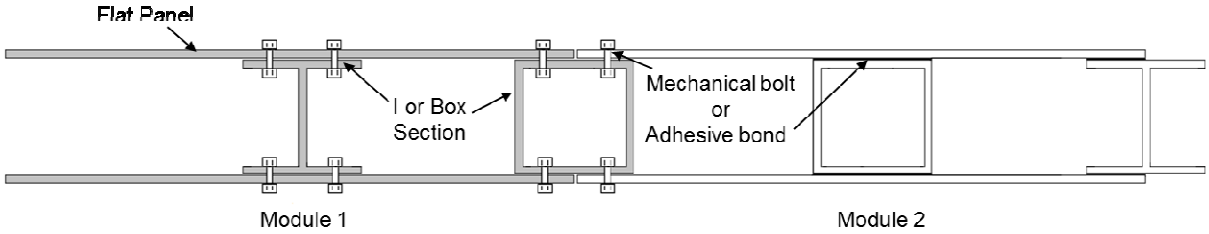


**Figure 1.** Proposed GFRP sandwich modular slab system assembled in the transverse direction

## EXPERIMENTAL INVESTIGATIONS

### Materials

Pultruded GFRP profiles (box sections supplied by Xingya FRP China and flat panels supplied by Exel Composites Australia) were used to fabricate a sandwich modular beam through adhesive bonding using Araldite 420 epoxy. Characterisation of the tensile properties of GFRP profiles was achieved by cutting out coupons from the box beams and flat panels with a water jet cutter, and then testing them in accordance with ASTM D3039. Coupons were cut from the rectangular flat panels in both the longitudinal and transverse directions, whilst only the longitudinal tensile properties were tested for the box beam samples. All coupons were 250 mm long and 25 mm wide. The width and thickness of each specimen were measured using a micrometre, and these dimensions were subsequently used to calculate the tensile strength and elastic modulus. Silicon Carbide sheets were used as the end-grips to avoid local failure at the specimen ends. Tensile testing was performed using an Instron 100kN-testing machine, with loads applied at a rate of 2mm/min. The longitudinal strain was measured with an LX500 laser extensometer with accuracy to 1 micrometre. The resulting material properties (as an average of those from 9 specimens) of the GFRP profiles are shown in Table 1. In addition, the material properties of the Araldite 420 epoxy adhesive are also provided in Table 1 according to the results given in Fawzia (2007).

**Table 1.** Material properties of GFRP profiles and epoxy adhesive

| Material | | Tensile Strength [MPa] | Tensile Modulus [GPa] | Shear strength [MPa] |
|---|---|---|---|---|
| Box Beams | Longitudinal | $281 \pm 11$ | $18.1 \pm 1.3$ | - |
| Flat Panels | Longitudinal | $293 \pm 20$ | $20.8 \pm 2.4$ | - |
| | Transverse | $88.1 \pm 5.1$ | $8.43 \pm 0.4$ | - |
| Araldite 420 epoxy (Fawzia, 2007) | | 28.6 | 1.9 | 25 |

### Specimen

A sandwich beam made from the above pultruded GFRP profiles was fabricated by adhesively bonding two box sections between two flat panels, as shown in Figure 2. The box beams were of size 102×102×5.3 mm, and the flat panels were 6 mm thick and 344 mm wide. The dimensions of the overall cross-section of the sandwich beam are shown in Figure 2. All profiles were cut to the appropriate size with a water jet cutter. The overall length of the beam was 2m and the span length was 1.65m. A 0.8mm-thick layer of Araldite 420 A/B epoxy adhesive was used to join the components together. The calculated EI of the sandwich beam considering the material properties given in Table 1 and a full composite action between the webs and face sheets is $3.7\times10^{11}$ Nmm$^2$. This value corresponds to 310% of the sum of the stiffness EI of the two box sections and two flat panels. The contribution of the adhesive layer was not included in the calculation due to its small thickness.

In order to ensure a good bond quality (and therefore a satisfactory composite action), all adherend surfaces were prepared in accordance with the procedure outlined in the Eurocomp Design Code and Handbook (Clarke, 1996). The adherend surfaces were first degreased with acetone and then sandblasted. The surfaces were degreased again just prior to bonding to remove any dirt. To control the thickness of the adhesive bond, spacer washers with a thickness of 0.8 mm were spaced in pairs at 400mm-intervals along each bonding surface. The two box beams were first bonded to the bottom panel and allowed to cure for one day before the application of the top panel. Weights were used to provide pressure whilst the adhesive cured, as shown in Figure 3a. The amount of adhesive was deemed adequate as there was generous squeeze-out in the joint during the bonding process (Figure 3b). The adhesive was cured for ten days at room temperature.

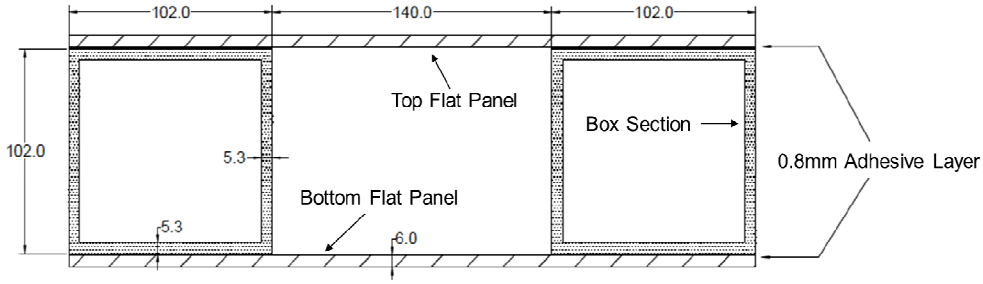


**Figure 2.** Dimensions of sandwich beam

**a)** **b)**

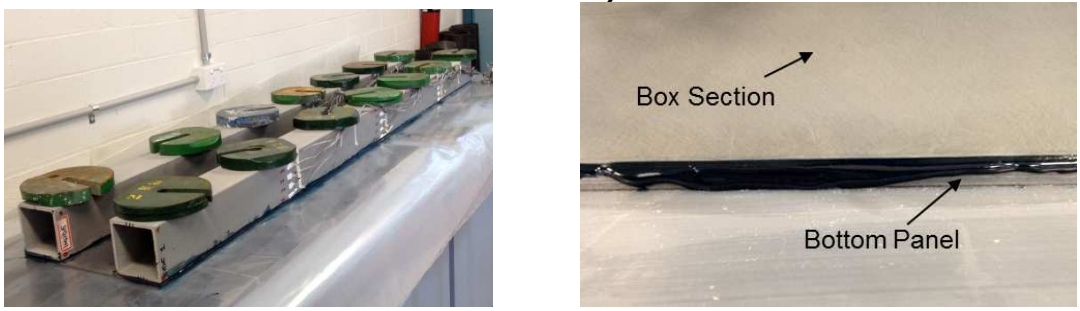


**Figure 3a)** Fabrication process of a sandwich beam with weights used to provide clamping pressure during curing of adhesive; **b)** Adhesive squeeze-out during bonding process

**Experiment Setup and Instrumentation**

The sandwich beam was simply supported and loaded in four-point bending with an Instron 100 kN Floating Actuator. As shown in Figure 4a, the point loads were transferred from the actuator through a distribution steel beam and applied to the specimen beam through two 350×50 $mm^2$ steel plates with a distance of span/3 from each support. A displacement control mode was adopted during the loading process at a rate of 1mm/min. The deflection was measured at midspan with a linear variable differential transducer (LVDT). 120-ohm-resistant strain gauges were placed in the longitudinal fibre direction along the top and bottom facesheets at midspan (see S1 to S5 and S26 to S30 in Figure 4b), and at a position of span/6 from the support (S6 to S10 and S31 to S35) to determine the axial strain distribution in the width direction. The span/6 position corresponds to a point halfway between the support and the point load, and hence measures the strain in the region of maximum shear. Strain gauges (S11-S25 and S36 to S40) were also placed in the longitudinal direction at midspan and at span/6 along the depth of the specimen in order to examine the assumption of 'plane sections remain plane'. Ten strain gauges (S41 to S50) were also applied along the depth of one of the inner-facing webs of a box section. All strain gauges were checked with an ohmmeter prior to testing to ensure that they functioned correctly. The load was applied in two steps. In the first, loading was applied up to 11 kN, which was the predicted serviceability load

for a deflection limit of span/300. Once the serviceability limit state (SLS) was reached, the beam specimen was unloaded at the same 1mm/min rate and then loaded up to failure.

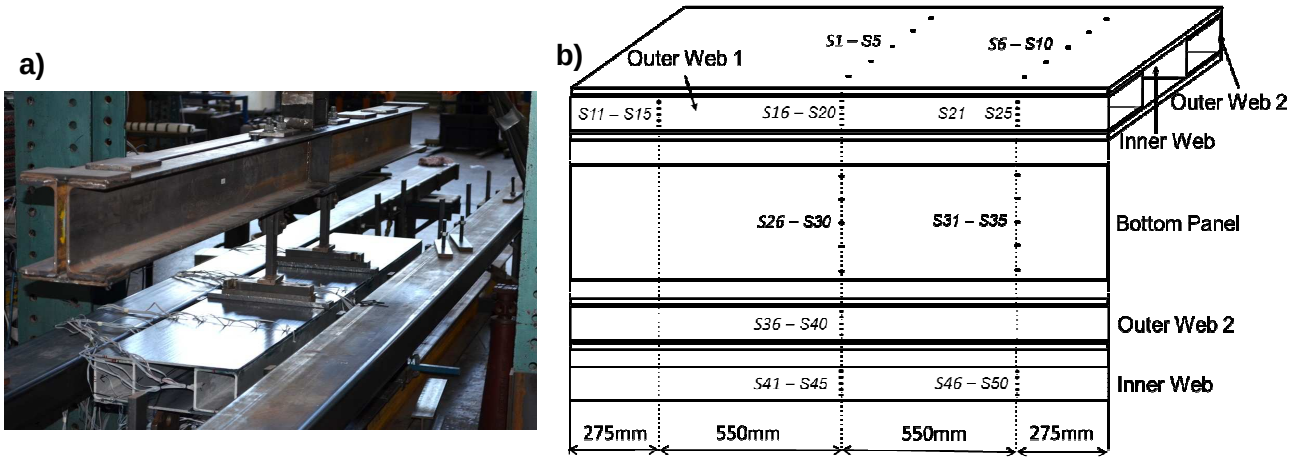


**Figure. 4a)** Experimental setup and **b)** strain gauge instrumentation

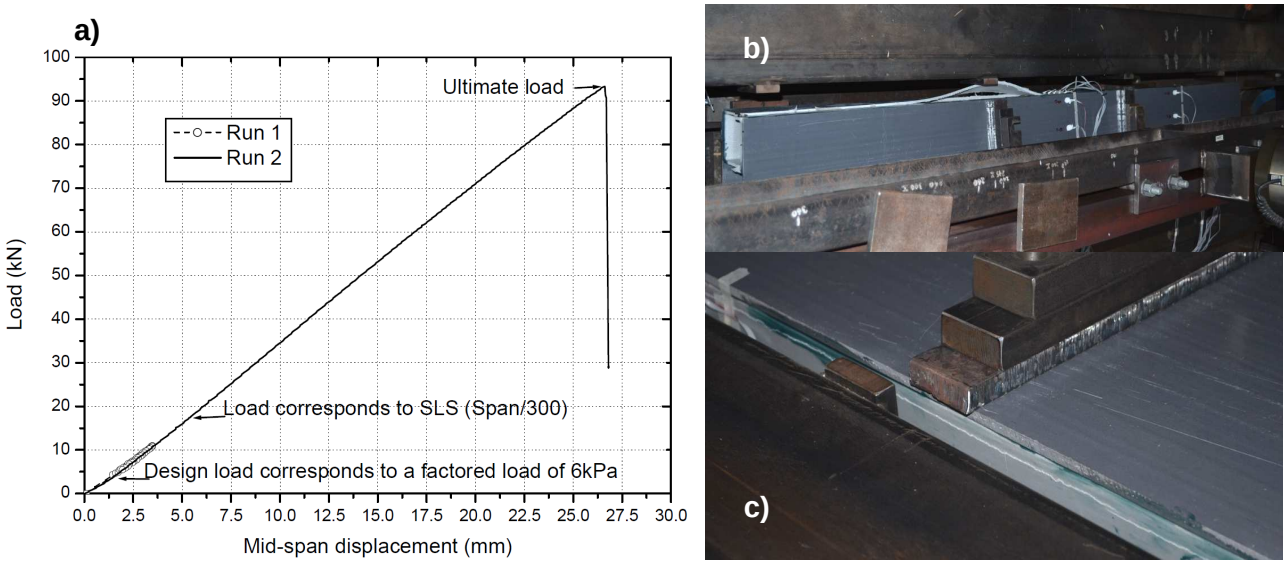


**Figure 5 a)** Load-displacement behaviour of sandwich beam at midspan; **b)** Shear failure at web-flange junction of one box section and **c)** of the other box section

## RESULTS AND DISCUSSION

### Load-deflection response and failure mode

The first load step (Run 1) was processed to a predicted SLS load of 11kN corresponding to a deflection limit of span/300. The load-deflection behaviour, as shown in Figure 5a, was linear up to the serviceability load. During the second load step (Run 2), whereby loads were applied up to failure, the load-deflection closely followed that from Run 1, indicating that there was no degradation to the stiffness of the beam during the first load run. Behaviour was also linear until brittle failure occurred at a load of 95kN (47.5kN for each point load). The bending stiffness EI, calculated from the load-displacement curve using Euler beam theory, was found to be $2.6\times10^{11}$ $Nmm^2$, corresponding to 70% of the calculated one given previously. This might be as a result of a lower material flexural modulus compared to the tensile modulus, or the shear deformation which is not taken into account in Euler beam theory. As shown in Figure 5a, the load-deflection curve also evidenced a large safety margin of ultimate load (95 kN) in comparison to the design load (3.4 kN

considering a factored uniformly distributed load of 6 kPa) and the SLS load (17 kN at 5.5 mm as span/300). Failure occurred via shearing of all the webs near the web-flange junction of the box sections, as shown in Figures 5b and 5c. Failure was sudden, with cracks initiating in the region of maximum shear and propagating rapidly within this region (from the support to the loading point, see Figure 5b). Due to such a shear crack, the web was separated from the face sheet of the box section and then easily buckled outwards near the loading point as shown in Figure 5b. The shear cracks arose at a position near the web-flange junction of the box sections as shown in Figure 5c. No failure was seen in the top or bottom panels, nor was it seen in the adhesive bond, indicating that the type of adhesive and the bonding technique utilised during fabrication was adequate.

**Axial strain along beam width**

The axial strains along the top panels (Figures 6a and 6b) and bottom panels (Figures 6c and 6d) were measured in order to characterise the distribution along the beam width. Measurements were taken at varying load levels up to the failure load P=95kN. The axial strains were fairly uniform along the beam width, indicating that the entire flat panel participated in bending in the areas of both shear (span/6 from support) and bending (midspan).

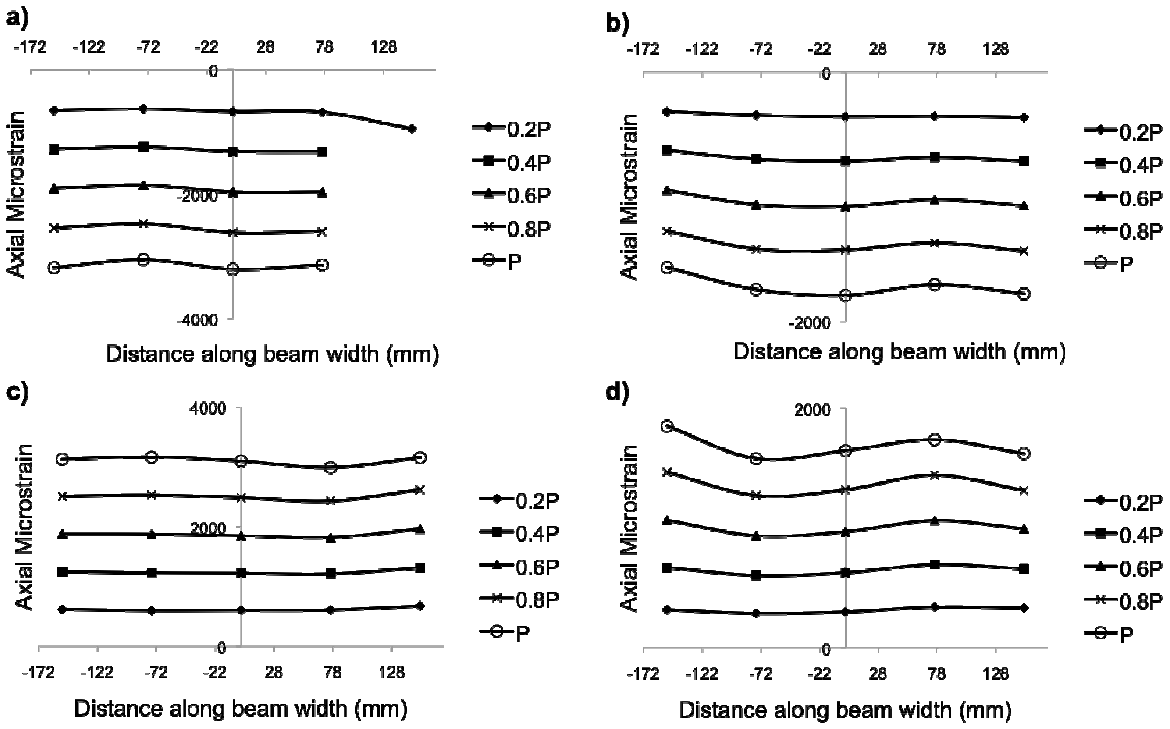


**Figure 6.** Axial strain distribution of **a)** the top facesheet at midspan (S1 to S5), **b)** the top facesheet at a distance span/6 from the support (S6 to S10), **c)** the bottom facesheet at midspan (S26 to S30) and **d)** the bottom facesheet at span/6 (S31 to S35).

**Axial strain along beam depth**

The connections between the FRP sections are important to ensure that load transfer between the components is efficient. The axial strain distribution along the beam depth for both the SLS load and failure load at midspan and at distance of span/6 are shown in Figures 7a and 7b respectively. As evidenced in these figures, differences in the strain distribution between the outer web and the inner web were negligible. In addition, the strain distribution measured at midspan on Outer Web 1 (strain gauges S16 to S20) was the same as that for Outer Web 2 (gauges S36 to S40 – not shown in Figure 7). As the axial strain distribution is linear from the top flat panel through the depth of the beam cross-section to the bottom flat panel, full composite action is provided by the adhesive

bonding. Furthermore, the strain distribution confirms the assumption that plane sections remain plane. These conclusions are valid for both serviceability and failure loads.

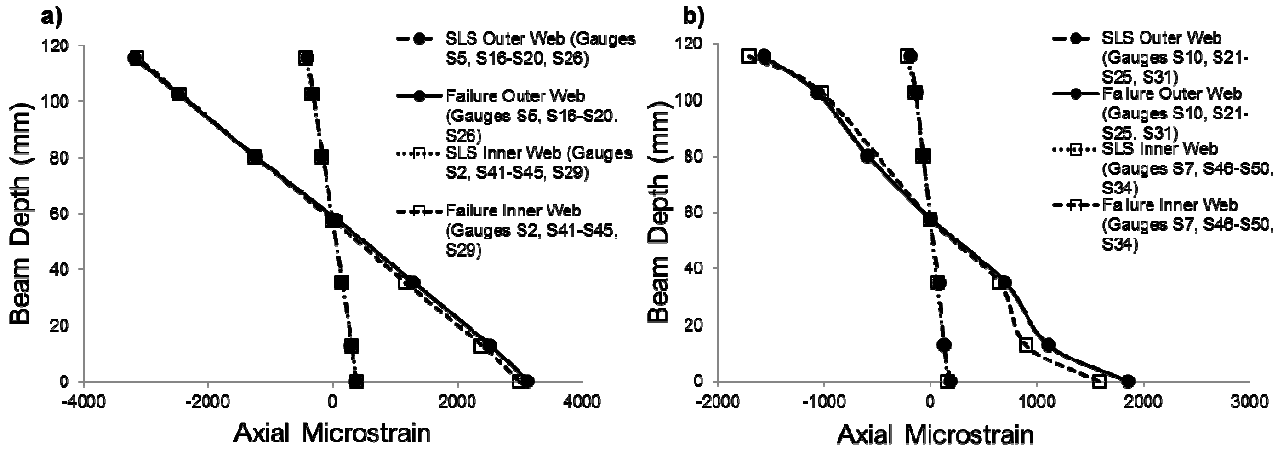


**Figure 7.** Axial strain distribution in cross-section at **a)** midspan and **b)** at span/6

**Shear stress analysis and failure prediction**

The elastic moduli of the panels and box-sections differ, and therefore the shear stress $\tau$ was calculated from Equation 1,

$$\tau = Q\frac{\int_A E(y)\cdot y\cdot dA}{b\cdot EI} \qquad (1)$$

where $Q$ is the shear force (i.e. 47.5 kN at failure), $E$ is the elastic modulus for the individual box or flat panel sections, $A$ is the cross-sectional area, $EI$ is the bending stiffness of the sandwich beam and $b$ is the width of the cross-section in shear. Figure 8 shows the maximum shear stress distribution at failure. The maximum shear stress was calculated as 28 MPa, occurring at the middle of the beam depth (i.e. the middle of web); however the web-flange junction of the box section also showed a shear stress of 25 MPa. The material shear strength, although not experimentally measured in this study (as planned in following experiments), was reported to be 27.6 to 34.5 MPa in general for pultruded GFRP materials (Borowicz and Bank, 2011). This suggests that the ultimate load carrying capacity and failure can be predicted in this way.

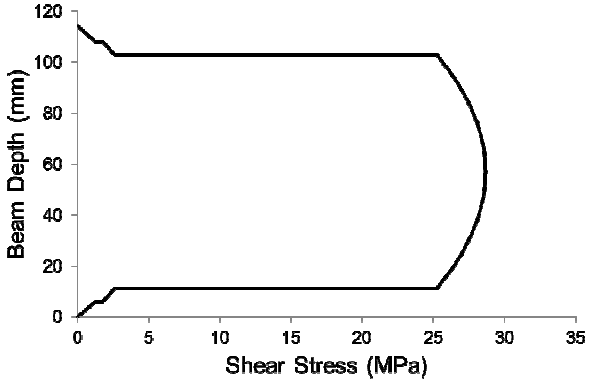


**Figure 8.** Shear stress distribution at failure load

## CONCLUSIONS

An innovative GFRP modular assembly system to enhance the bending stiffness of GFRP structures was introduced in this paper. A sandwich beam, consisting of two pultruded box beams sandwiched between flat panels, was fabricated and tested under four-point bending. The beam displayed linear behaviour up to failure at 95 kN. Failure was sudden, occurring at the web-flange junction of the box sections due to shear. Strain results evidenced that the whole flat panel participated in bending

equally and full composite action was provided by the adhesive bond. This also suggested that adhesive bonds are a viable means of connecting GFRP components together in sandwich construction. The work indicates that all-composite GFRP sandwich structures behave favourably in terms of their structural performance. These sandwich structures may be adapted to form modular slab sections, which can then be assembled in the transverse direction via adhesive bonding and/or mechanical bolting. Such systems appear to have great potential in structural construction.

## ACKNOWLEDGEMENT

The author wishes to acknowledge Mr. Long Goh, Mr. Kevin Nievaart and Mr Mark Taylor for their assistance in conducting the experiments at the Monash Structural Laboratory. Financial support was received from the Australian Research Council through the Discovery Early Career Researcher Award scheme and Monash University. The GFRP materials were supplied by Xingya FRP China and Exel Composites, Australia.

## REFERENCES

ASTM D3039-00, Standard Test Method for Tensile Properties of Polymer Matrix Composite Materials.

Bakis, C. E., Bank, L. C., Brown, V. L., Cosenza, E., Davalos, J. F., Lesko, J. J., Machida, A., Rizkalla, S. H. and Triantafillou, T. C. (2002). Fiber-Reinforced Polymer Composites for Construction - State-of-the-Art Review. *Journal of Composites for Construction* **6**(2): 73-87.

Borowicz DT and Bank LC. Behavior of pultruded fiber-reinforced polymer beams subjected to concentrated loads in the plane of the web. *ASCE Journal of Composites for Construction 2011*, **15**(2): 229-238

Clarke, J. L. (1996). *Structural design of polymer composites: EUROCOMP design code and handbook*, E & FN Spon.

Davalos, J. F., Chen, A. and Zou, B. (2011). "Stiffness and Strength Evaluations of a Shear Connection System for FRP Bridge Decks to Steel Girders " *Journal of Composites for Construction* **15**(3): 441-450.

Fawzia, S. (2007). *Bond Characteristics between Steel and Carbon Fibre Reinforced Polymer (CFRP) Composites*. PhD, Monash University.

Foster, D. C., Richards, D. and Bogner, B. R. (2000). "Design and Installation of Fiber-Reinforced Polymer Composite Bridge." *Journal of Composites for Construction* **4**(1): 33-37.

Halliwell, S. (2010). "Technical Papers: FRPs — The Environmental Agenda." *Advances in Structural Engineering* **13**(5): 783-791.

Hayes, M. D., Ohanehi, D., Lesko, J. J., Cousins, T. E. and Witcher, D. (2000). "Performance of Tube and Plate Fiberglass Composite Bridge Deck." *Journal of Composites for Construction* **4**(2): 48-55.

Jeong, J., Lee, Y.-H., Park, K.-T. and Hwang, Y.-K. (2007). "Field and laboratory performance of a rectangular shaped glass fiber reinforced polymer deck." *Composite Structures* **81**(4): 622-628.

Johnson, A. F., Sims, G. D. and Ajibade, F. (1990). "Performance analysis of web-core composite sandwich panels." *Composites* **21**(4): 319-324.

Keelor, D. C., Luo, Y., Earls, C. J. and Yulismana, W. (2004). "Service Load Effective Compression Flange Width in Fiber Reinforced Polymer Deck Systems Acting Compositely with Steel Stringers." *Journal of Composites for Construction* **8**(4): 289-297.

Keller, T. and Gürtler, H. (2005a). "Composite Action and Adhesive Bond between Fiber-Reinforced Polymer Bridge Decks and Main Girders." *Journal of Composites for Construction* **9**(4): 360-368.

Keller, T. and Gürtler, H. (2005b). "Quasi-static and fatigue performance of a cellular FRP bridge deck adhesively bonded to steel girders." *Composite Structures* **70**(4): 484-496.

Liu, Z., Majumdar, P. K., Cousins, T. E. and Lesko, J. J. (2008). "Development and Evaluation of an Adhesively Bonded Panel-to-Panel Joint for a FRP Bridge Deck System." *Journal of Composites for Construction* **12**(2): 224-233.

Moon, F. L. and Gillespie, J. J. W. (2005). "Experimental Validation of a Shear Stud Connection between Steel Girders and a Fiber-Reinforced Polymer Deck in the Transverse Direction." *Journal of Composites for Construction* **9**(3): 284-287.

Sotiropoulos, S. N., GangaRao, H. V. S. and Mongi, A. N. K. (1994). "Theoretical and Experimental Evaluation of FRP Components and Systems." *Journal of Structural Engineering* **120**(2): 464-485.

Turner, M. K., Harries, K. A., Petrou, M. F. and Rizos, D. (2004). "In situ structural evaluation of a GFRP bridge deck system." *Composite Structures* **65**(2): 157-165.

Zhou, A., Coleman, J. T., Temeles, A. B., Lesko, J. J. and Cousins, T. E. (2005). "Laboratory and Field Performance of Cellular Fiber-Reinforced Polymer Composite Bridge Deck Systems." *Journal of Composites for Construction* **9**(5): 458-467.